Onset of continuous wave Nd:YAG and argon laser tissue ablation

Verdaasdonck, Rudolf, Borst, Cornelius, van Gemert, Martin

Rudolf M. Verdaasdonck, Cornelius Borst M.D., Martin J. C. van Gemert, "Onset of continuous wave Nd:YAG and argon laser tissue ablation," Proc. SPIE 1202, Laser-Tissue Interaction, (1 June 1990); doi: 10.1117/12.17624

SPIE.

Event: OE/LASE '90, 1990, Los Angeles, CA, United States

Onset of continuous wave Nd:YAG and Argon laser tissue ablation

*Rudolf M. Verdaasdonk, Cornelius Borst, Martin J. C. van Gemert**

Experimental Cardiology Laboratory, Heart Lung Institute, University Hospital Utrecht, Utrecht,
**Medical Laser Laboratory, Academic Medical Centre, Amsterdam, The Netherlands*

ABSTRACT

To study the onset of tissue ablation by cw laser irradiation, aortic and myocardial bovine tissue samples were exposed in air to a 1 mm diameter laser beam of either 15 W Nd-YAG or 3.5 W Argon. Exposure times varied from 0.1 to 30 s. The surface of the tissue was filmed with a resolution of 0.01 mm and recorded on video with time coding. A photodiode positioned underneath the tissue samples measured forward transmitted light. After exposure the tissue was processed for histology. The observed phenomena were divided in three phases: Phase A: The tissue surface slightly discolored while the transmission signal remained constant or slightly diminished. Phase B: Simultaneous with a 'pop' sound, the surface rose and the transmission dropped abruptly to about 50 % and remained at this level for several seconds during vaporization of tissue water. Histology showed ruptured layers and multiple vacuoles beneath the surface. Phase C: In the middle of the beam a spot of carbonized tissue was formed which grew concentrically from the center while a crater was formed. No drop in the transmission was observed when carbonization started. On the crater bottom carbonization and vaporization followed in rapid succession while light transmission increased. Histology showed along the crater edge a 20 µm thick layer of carbonization and a 200 µm thick layer of vacuoles due to tissue water boiling whereas on the crater bottom these layers were only 10 and 20 µm thick respectively. Thus, the small zone of vacuoles at the crater bottom suggest that a large temperature gradient existed at the ablation front.

The 'popcorn' phenomenon is attributed to the explosive formation of vapor bubbles underneath the tissue surface caused by the anatomically or heat-induced layered structure of the tissue resulting in enhanced reflection and scattering of the laser light due to multiple tissue-vapor transitions.

1. INTRODUCTION

Light-tissue interaction is a complex process. Depending on the optical properties of the tissue and the diameter of the beam, light is scattered and absorbed during tissue irradiation by a continuous wave laser. The absorbed light heats the tissue which results in changes of the tissue properties. These changes influence the onset and progression of the tissue ablation proces. This study examines tissue changes during initiation of tissue ablation by continuous wave lasers. Close-up videorecording was used to analyze macroscopic changes at the tissue surface, forward light transmission was measured to detect changes in optical properties of the tissue and histology was obtained to assess microscopic changes of the tissue at various stages of the initiation of ablation.

2. METHODS

2.1 Tissue specimens

Bovine aortic and cardiac tissue samples, up to 8 mm thick, were obtained within 24 hours after death and stored in saline at 4 °C. The endocardium and epicardium were removed from the myocardium prior to irradiation.

2.2 Laser protocol

In air, a 10 degree divergent laser beam was focused perpendicularly on the surface of a tissue sample by means of a lens which produced a long waist of 1 mm diameter near the focal point. The laser sources used were an Argon ion laser (wavelength 488/514.5 nm, Innova 30, Coherent, Palo Alto, USA) at 3.5 W (4.5 W/mm^2) and a continuous wave Nd:YAG laser (wavelength 1064 nm, MD 60, Surgical Laser Technologies, Malvern, USA) at 10 W (13 W/mm^2) and 15 W (19 W/mm^2). Exposure times varied from 0.1 to 30 seconds. The aortic specimens were irradiated from both the intimal and the adventitial side. To "freeze" particular stages during the ablation process, the laser was switched off at moments of interest.

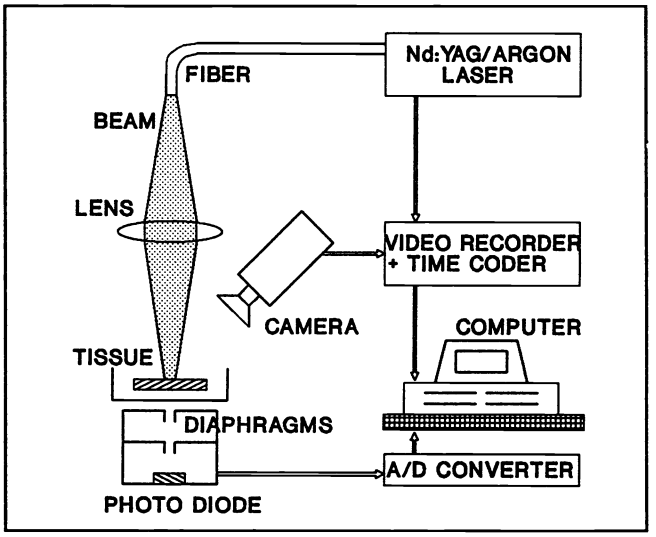

Figure 1
Diagram of the setup. A 1 mm diameter waist of a laser beam was focussed on the surface of a tissue sample. Changes at the surface where recorded on video and changes in the forward transmitted light intensity were measured by a photodiode simultaneously. The signals were sampled with 25 Hz and coded with a time signal.

2.3 Video recording of crater formation

During laser exposure the surface of the tissue was filmed and recorded on video through an operating microscope (Opmi-99, Zeiss, FRG). A tissue area of 3 mm across could be studied with a spatial resolution of 10 µm. Each individual video frame was coded with a stopwatch time signal which was started simultaneously with the laser. The time interval between the frames was 0.04 seconds (25 Hz). In case of Argon laser light, the high intensity back-scattered light from the tissue surface was filtered by means of an argon safety goggle in front of the camera lens.

2.4 Light transmission

A photodiode was positioned in the beam path underneath the tissue to measure light transmitted through the tissue sample. Two diaphragms with an aperture of 1 mm diameter were positioned between the tissue sample and the photodiode to reduce the contribution of scattered light to the transmission signal. The transmission signal was A/D converted with a sample frequency of 25 Hz, coincident with the video frames and recorded by computer (fig. 1).

2.5 Histology

After exposure, the tissue samples were fixed and processed for light microscopy by standard methods with the Hematoxylin and Eosin and the Weigert van Gieson's elastin staining.

3. RESULTS

3.1 Ablation phases

During initiation of tissue ablation three different phases were distinguished. These three phases are illustrated in figure 2 which shows representative transmission-time signals during the ablation process. The composition of video frames in figure 3 shows sequential moments during tissue ablation. Relevant histology is presented in figure 4. The three phases were observed with aortic and myocardiac tissue with either laser wavelengths. The data are presented in table 1.

phase A :

The transmission through aorta decreased slightly (fig. 2A) but transmission through myocardium decreased about 30 % (fig. 2B). The tissue surface discolored and in some cases it moved a few tenths of a millimeter due to shrinkage. Histologically, no distinct thermal damage was found.

phase B :

Coincident with a 'pop' sound a rise of the tissue surface was seen within the time interval between two video frames (0.04 s) (fig. 3A,B) while the transmission signal dropped abruptly to about 50 % of its initial level. It remained at this level untill the onset of phase C (fig. 2A,B). The surface moved suggesting the presence of boiling bubbles underneath. When the laser was switched off immediately after the pop sound, the tissue showed ruptured layers and multiple vacuoles beneath the surface down to a depth of 300 µm (fig. 4A). In some cases both the 'pop' sound and the coincident drop in light transmission did not occur (table 2).

phase C :

The formation of a small black spot on the tissue in the center of the beam (fig. 3C) initiated tissue carbonization. Within tenths of seconds the centre spot cleared changing into a ring (fig. 3D) which grew concentrically from the center while a crater was formed (fig. 3D-F, 4B). On the bottom of the crater concentric rings of carbonization and vaporization followed each other in rapid succession. The expanding rings of carbonized tissue were deposited at the crater wall while the tissue was ablated. In almost all cases the intensity of the transmitted light did not decrease at the onset of tissue carbonization (fig. 2A,B). While tissue carbonization and vaporization proceeded, light transmission increased untill the saturation level of the photodiode was reached. Along the crater edge a 20 µm layer of carbonization and a 200 µm zone of vacuoles were found (fig. 4C). On the bottom of the crater, however, these layers were only 10 and 20 µm thick, respectively (fig. 4C).

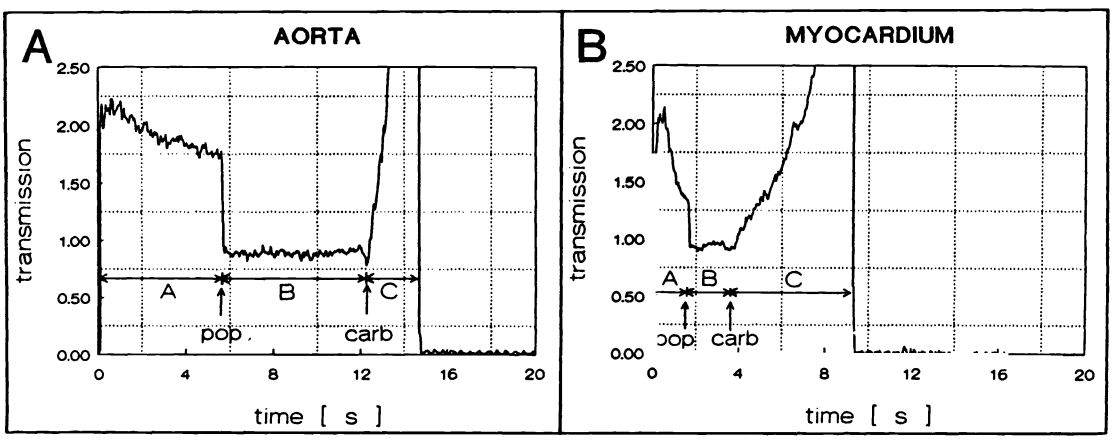

Figure 2 : Forward light transmission changes (arbitrary units) at the onset of tissue ablation of aorta (A) and myocardium (B). 'A' is the period from start laser exposure till explosive vaporization ('pop') occurred, 'B' is the period between 'pop' and moment of carbon formation on the tissue surface ('carb') and during period 'C' the ablation crater is formed while tissue is vaporized. Both examples are during Nd:YAG irradiation (19 and 13 W/mm^2 resp.) perpendicular to the tissue.

Table 1. Experimental data

laser/tissue combination	duration				'pop" occurence		transmission decrease		power density
	phase A		*phase B*				*phase A*	*phase B*	
	sec	*sd*	*sec*	*sd*	*%*	*n*	*% (sd)*	*% (sd)*	*W/mm²*
Nd:YAG / aorta, interna	15.0	4.2	2.0	0.8	90	22	<5	54 (8)	19
Nd:YAG / aorta, adventitia	-	-	-	-	25	8	<5	50 (5)	19
Nd:YAG / myocard	4.7	0.6	4.2	1.5	73	22	25 (5)	28 (8)	13
Argon / aorta, interna	0.9	0.3	1.5	0.4	60	23	<5	50	4.5
Argon / aorta, adventitia	-	-	-	-	0	6	-	-	4.5
Argon / myocard	0.25	0.04	0.21	0.04	66	15	-	-	4.5

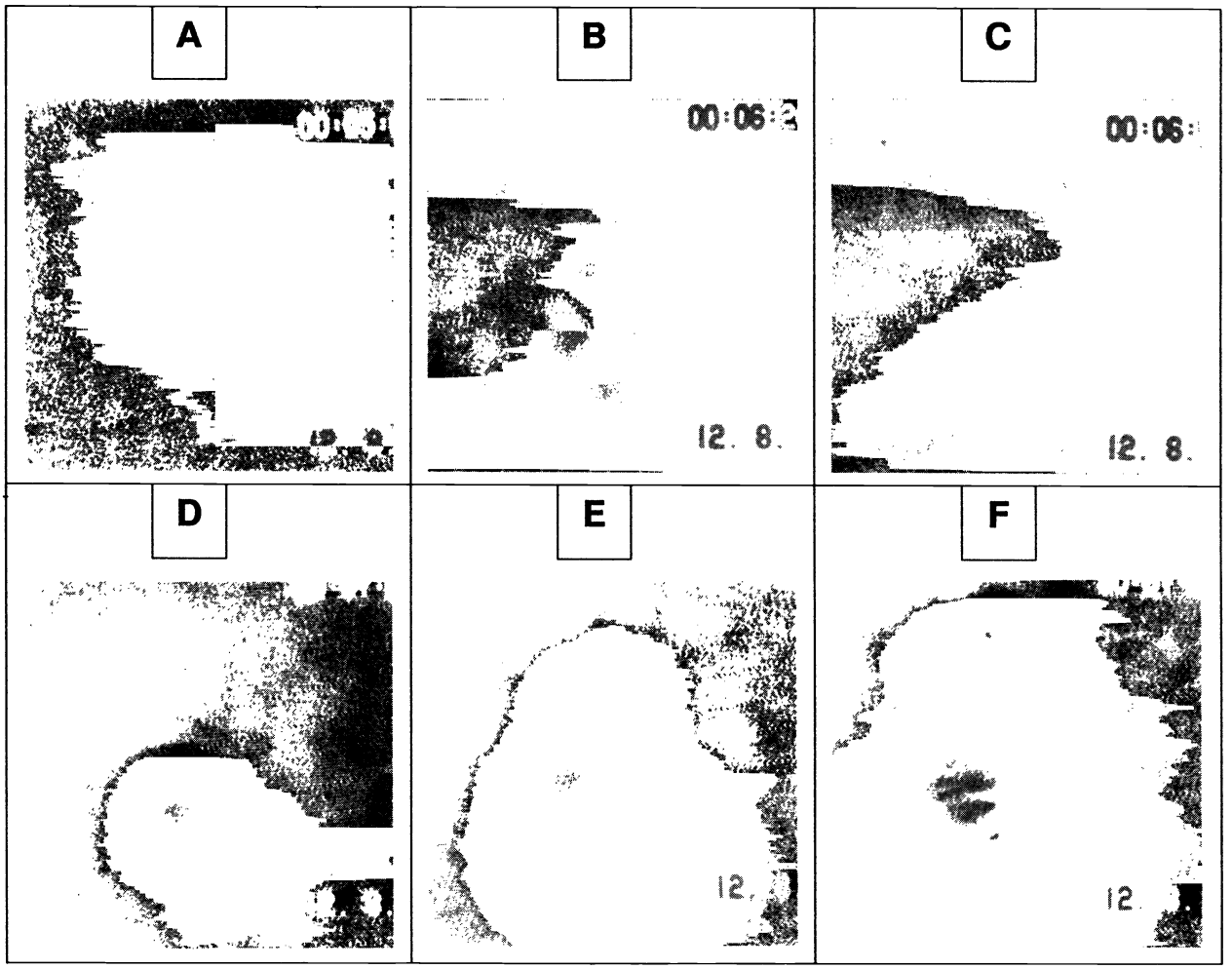

***Figure 3** : Composition of video frames at successive stages of the initial ablation proces. (A) the surface of aortic tissue shows no changes 5.97 s after the start of exposure with Nd:YAG laser light. (B) After 6.24 s, explosive evaporation was accompanied by the 'pop' sound. Bubbles in the tissue pushed the surface up. (C) A spot of carbonized tissue was formed in the centre at 6.88 s. (D,7.08 s), (E, 7.44 s) to (F, 7.84 s) The carbonized spot grew into a ring shape while its centre became clear again. The bottom of the crater carbonized and cleared in a cyclic fashion during the progression of crater formation.*

3.2 duration pre-ablation phases

The duration of the pre-ablation phases A and B were determined from the light transmission signal or video recordings if transmission was too low (Argon/myocard). For most laser/tissue combinations the pre-ablation phases lasted a few seconds, whereas the pre-ablation phases in case of Argon/myocard lasted less than 0.5 second (table 1).

3.3 incidence of the 'pop' sound

The incidence of the 'popcorn' phenomenon (start of phase B) is listed in table 1. The 'pop' sound was heard in two thirds of the observations. Its occurrence depended on the tissue and the laser type. Only in case of aorta irradiated from the adventitial side in air the 'pop' sound was less frequent.

3.4 transmission

Light transmission of Argon light through myocard could not be measured due to its high absorption.

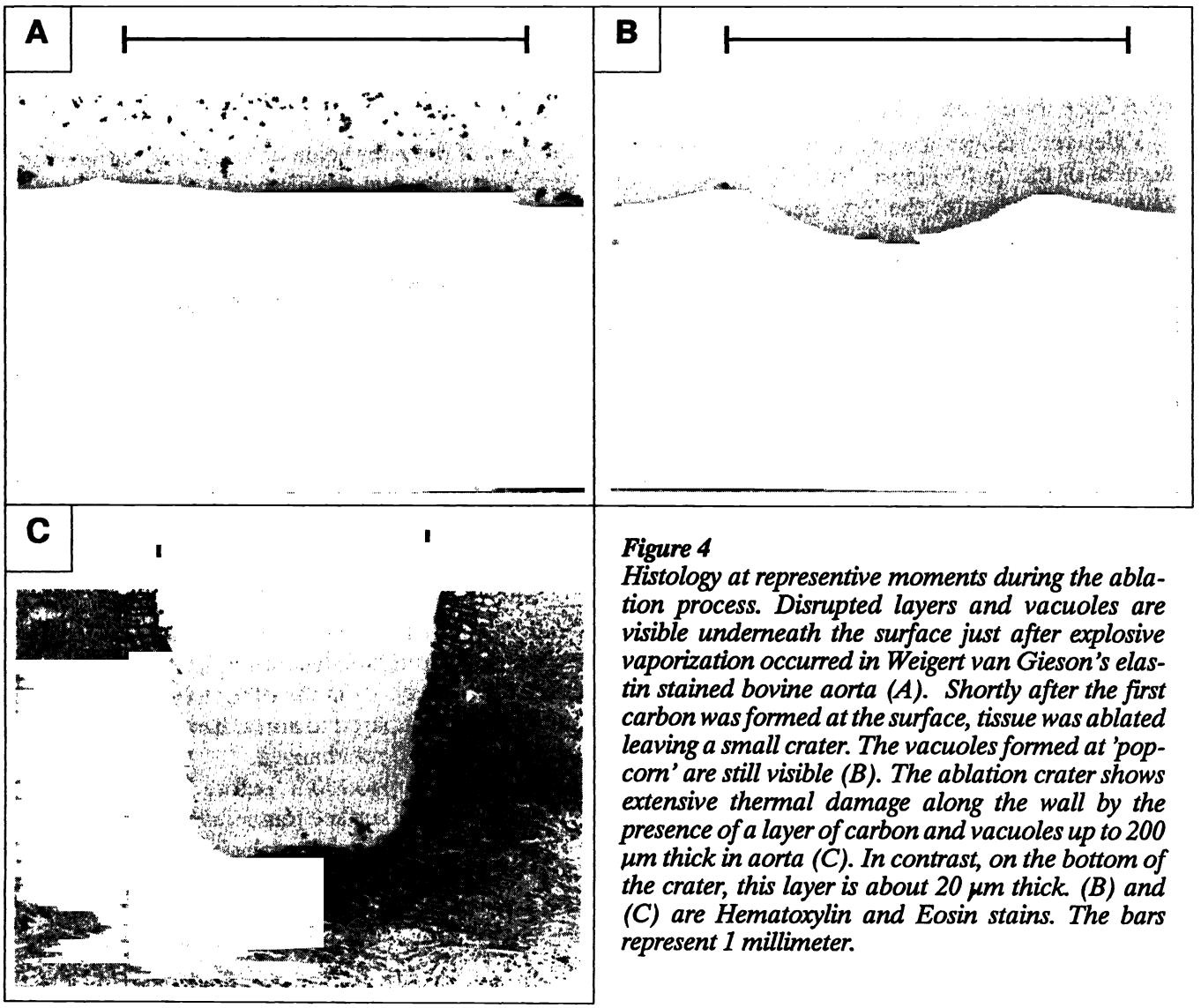

Figure 4
Histology at representive moments during the ablation process. Disrupted layers and vacuoles are visible underneath the surface just after explosive vaporization occurred in Weigert van Gieson's elastin stained bovine aorta (A). Shortly after the first carbon was formed at the surface, tissue was ablated leaving a small crater. The vacuoles formed at 'popcorn' are still visible (B). The ablation crater shows extensive thermal damage along the wall by the presence of a layer of carbon and vacuoles up to 200 μm thick in aorta (C). In contrast, on the bottom of the crater, this layer is about 20 μm thick. (B) and (C) are Hematoxylin and Eosin stains. The bars represent 1 millimeter.

4. DISCUSSION

4.1 EXPLOSIVE VAPORIZATION ('POPCORN')

The explosive vaporization of water of biological tissue resulting in the 'popcorn' phenomenon has been described as laser-induced decrepitation by Langerholc in 1979 [1,2]. More aspects of the phenomenon have been reported more recently [3,4].

4.1.1 Bubble formation

The 'pop' sound is attributed to the sudden formation of vapour below the tissue surface. The structure of the tissue can prevent the formation of vapour bubbles when tissue water temperature rises to above boiling temperature. But when the vapour pressure associated with the temperature of the overheated water exceeds the internal pressure accommodated by the tissue structure, superheated vapour bubbles are generated abruptly. The vapour pressure increases exponentially with temperature and is already near 5 bar at 150 °C [5]. The surface rise and the bubble underneath are clearly seen in fig. 3B.

4.1.2 Light transmission decrease

Video recordings showed a increase in brightness of the spot of the laser beam on the tissue surface at the moment of the 'pop'. Figure 4A,B shows the presence of the vacuoles and the disrupted tissue layers within tenths of seconds after the 'pop' occurred. These abruptly formed vapour bubbles and ruptures in the tissue are likely to reflect and scatter light at every transition of vapour and tissue resulting in enhanced scattering and reflection. This could explain the dip to about 50 % of its initial intensity observed in the transmission signal simultaneous with the 'pop' (fig. 2).

4.1.3 Mechanism of 'popcorn'

Explosive subsurface vaporization could be induced when boiling temperature is reached first below the surface. This condition is created when the light fluence is highest subsurface resulting in greater heat generation due to absorption. One dimensional light propagation models predict this situation [3] but the existence of the highest light fluence subsurface is ambiguous in three dimensional models [6].

Cooling at the surface could also result in higher subsurface temperatures. This situation has been modeled for laser ablation of solids resulting in the prediction of explosive ablation [7]. It is uncertain if this theory can be applied to tissues.

The 'popcorn' phenomenon may also be related to the layered structure of tissue. This explanation is supported by the higher incidence of 'popcorn' when irradiating aorta from the structurally layered luminal side in contrast to the more homogeneously structured adventitial side (table 1). On the other hand, 'popcorn' did also occur in the homogeneous myocardium though less pronounced compared to aorta. It is also possible that due to dehydration during tissue irradiation the structure of the surface layer changed.

In a recent paper LeCarpentier et al. [4] reported surface temperatures up to 150 °C before the 'pop' occurred measured in conditions similar to our experiments. This suggests that the surface temperature is not clamped at boiling temperature. A surface temperature of 150 °C would be compatible with a dehydrated and denatured surface layer of diminished compliance that acts as a structural barrier to subsurface tissue water boiling. Eventually, explosive subsurface vaporization starts.

4.2 CARBONIZATION AND CRATER FORMATION

4.2.1 Absence of transmission dip

Absorption increases dramatically at the very moment tissue turns black due to carbon formation. Consequently, light transmission is expected to drop. At the onset of carbonization, as observed on the videoframes (fig. 3), the expected abrupt drop in forward transmission was usually not observed (fig. 2, 'carb'). Probably the surface area of the initial spot of carbonization (fig. 3C) and the later ring (fig. 3D-F) are only small in comparison to the total area irradiated by the beam. This would explain why, within the error of measurement, no decrease was measured in the forward light transmission. In a few cases when a small dip in the transmission signal was found, the video recordings showed either the presence of a dark plume or a large piece of carbonized tissue in the centre of the beam.

4.2.2 Cyclic carbonization

During crater formation rings of carbonized layers moved across the bottom of the crater starting in the centre heading to the edges in a cyclic way. Acute thermal damage was most pronounced near the wall whereas it was almost absent at the bottom. The layer of carbonization was about 20 μm and the layer of vacuoles was about 200 μm at the crater wall in contrast to a 10 μm layer of carbonization and a 20 μm layer of vacuoles at the bottom. This suggest the existence of steep temperature gradient over the crater bottom to the underlaying tissue. The phenomenon that the bottom turns black and clears again in a rapid cycle suggests a fast oscillation between temperatures above tissue vaporization and temperatures below tissue carbonization. The maximum temperatures reached during tissue ablation are difficult to measure. Temperatures between 220 and 350 °C [4,8] have been measured with thermocameras during the ablation of plaque but temperatures up to 1000 °C have been suggested [9,10]. Light emission observed during tissue ablation with optical angioplasty probes such as ball-shaped fibers (unpublished data, Verdaasdonk et al.) also indicate temperatures of up to 1000 °C.

4.3 Thermal tissue damage

In vitro tissue damage due to heat exposure below 100 °C is difficult to assess with standard histology staining techniques. Protein denaturation manifests itself most clearly in vivo by cell necrosis after one or more days. Because of this the total extent of tissue damage mostly due to heat conduction could not be determined.

5. CONCLUSIONS

Continuous wave laser ablation of tissue by Nd:YAG or Argon laser irradiation can be divided in three phases:

Phase A: tissue discoloring and shrinkage due to denaturation of proteins and dehydration during a surface temperature increase to about 150 °C.

Phase B: explosive subsurface vapour formation ('popcorn') resulting in enhanced scattering and reflection at multiple tissue-vapour transitions followed by tissue water boiling

Phase C: tissue carbonization and vaporization in a cyclic fashion. Carbonization did not influence the forward transmission.

The 'popcorn' phenomenon is most likely related to the layered structure of the tissue and/or to the laser induced structure changes of the surface of the tissue.

A 20 μm thermal damage zone at the bottom of the ablation crater in contrast to an 200 μm zone along the crater wall suggests a large temperature gradient along the tissue ablation front.

6. ACKNOWLEDGEMENTS

We thank F. W. Cross, MD, A. J. Welch, PhD, M. Motamedi, PhD and S. L. Jacques, PhD for their comments on the manuscript. We thank E. Velema for the histology and S. L. Thomsen, MD and L. van Erven, MD for their help in interpreting the histology.

7. REFERENCES

1. J. Langerholc, " Moving phase transitions in laser-irradiated biological tissue", *Applied Optics*, 18, pp. 2286-2293, 1979.
2. T. Halldorsson, J. Langerholc, L. Senatori and H. Funk, " Thermal action of laser irradiation in biological material monitored by egg-white coagulation", *Applied Optics*, 20, pp. 822-825, 1981.
3. S. L. Jacques and S. A. Prahl, " Modeling optical and thermal distributions in tissue during laser irradiation", *Lasers.Surg.Med.*, 6, pp. 494-503, 1987.
4. G. L. LeCarpentier, M. Motamedi, S. Rastagar and A. J. Welch, " Simultaneous analysis of thermal and mechanical events during CW laser ablation of biological media", *Proceedings SPIE*, 1068, 1989.
5. R. C. 5. Weast, CRC Handbook of Chemistry and Physics, pp. D-193, CRC Press, Boca Raton, 1984.
6. G. Yoon, A. J. Welch, M. Motamedi and M. J. C. van-Gemert, " Development and application of three-dimensional light distribution model for laser irradiated tissue", *IEEE J. Quantum Electron.*, QE-23, pp. 1721-1733, 1987.
7. F. W. Dabby and U. C. Paek, " High-intensity laser-induced vaporization and explosion of solid material", *IEEE J. Quantum Electron.*, QE-8, pp. 106-111, 1972.
8. A. J. Welch, J. W. Valvano, J. A. Pearce, L. J. Hayes and M. Motamedi, " Effect of laser radiation on tissue during laser angioplasty", *Lasers Surg Med*, 5, pp. 251-264, 1985.
9. G. Laufer, " Primary and secondary damage to biological tissue induced by laser irradiation", *Applied Optics*, 22, pp. 676-681, 1983.
10. N. P. Furzikov, " Different lasers for angioplasty: thermooptical comparison", *IEEE J. Quantum Electron.*, QE-23, pp. 1751-1755, 1987.